Journal of Central South University, Volume 31, Issue 7, July 2024, pp. 2181-2193
DOI: 10.1007/s11771-024-5740-2

Springer

Effect of thermo-mechanical treatment on microstructure and mechanical properties of wire - arc additively manufactured Al-Cu alloy

Tao ZHANG(张涛)[1,2], Zhen-yang QIN(秦振洋)[1,2], Hai GONG(龚海)[1,2,*], Yun-xin WU(吴运新)[1,2], Xin Chen[3]

[1] Light Alloy Research Institute, Central South University, Changsha 410083, China
[2] State Key Laboratory of Precision Manufacturing for Extreme Service Performance, Central South University, Changsha 410083, China
[3] Welding and Additive Manufacturing Centre, Cranfield University, Bedford, MK43 0AL, UK

© Central South University Press 2022

Abstract: Wire - arc additive manufacture (WAAM) has great potential for manufacturing of Al-Cu components. However, inferior mechanical properties of WAAM deposited material restrict its industrial application. Inter-layer cold rolling and thermo-mechanical heat treatment (T8) with pre-stretching deformation between solution and aging treatment were adopted in this study. Their effects on hardness, mechanical properties and microstructure were analyzed compared to the conventional heat treatment (T6). The results show that cold rolling increases the hardness and strengths, which further increase with T8 treatment. The UTS of 513 MPa and YS of 413 MPa can be obtained in the inter-layer cold-rolled sample with T8 treatment, which is much higher than that in the as-deposited samples. The cold-rolled samples show higher elongation than that of as-deposited ones due to significant elimination of porosity in cold rolling; while both the T6 and T8 treatments decrease the elongation. The cold rolling and pre-stretching deformation both contribute to the formation of dense and dispersive precipitated θ′ phases, which inhibits the dislocation movement and enhances the strengths; as a result, T8 treatment shows better strengthening effect than the T6 treatment. The strengthening mechanism was analyzed and it was mainly related to work hardening and precipitation strengthening.

Key words: Wire - arc additive manufacture; inter-layer cold rolling; thermal-mechanical treatment; microstructure; mechanical properties; strengthening mechanism

Cite this article as: Tao ZHANG, Zhen-yang QIN, Hai GONG, Yun-xin WU, Xin Chen. Effect of thermo-mechanical treatment on microstructure and mechanical properties of wire - arc additively manufactured Al-Cu alloy [J]. Journal of Central South University, 2022, 29(): . DOI:

1 Introduction

Al-Cu alloy is widely used in aerospace field with the advantages of light weight, high specific strength, excellent weldability and low-temperature performances (-270℃~300℃) [1]. Al-Cu alloy is the key material of aerospace components, such as fuel tanks of launch rocket, fuselage and skin of supersonic aircraft and cryogenic tanks [2]. Wire - arc additive manufacture (WAAM) has great potential for the manufacturing of key components in aerospace [3-4]. However, inferior mechanical properties of the WAAM deposited material in comparison with wrought components restrict its application in industry [5-6].

Al-Cu alloy is a type of precipitation strengthened alloy, and the solution and artificial aging heat treatment (T6) is essential for the strengths enhancement [7]. The alloying elements

Foundation item: Project (ZZYJKT2021-05) supported by the State Key Laboratory of Precision Manufacturing for Extreme Service Performance, Central South University; Project (201806835007) supported by China Scholarship Council.
Received date: 0000-00-00; **Accepted date:** 0000-00-00
Corresponding author: Hai GONG; Email: gonghai@csu.edu.cn; ORCID: 0000-0003-2913-5382

Published by Springer. This is the Author Accepted Manuscript.
The final published version (version of record) is available online at DOI:10.1007/s11771-024-5740-2. Please refer to any applicable publisher terms of use.

are dissolved and supersaturated solid solution is generated during the solution treatment; meanwhile, the strengthening particles (Al-Cu eutectics) precipitate into the matrix during the subsequentaging process. For Al-Cu alloy, the sequence of the precipitation is described as follows: Guinier-Preston (GP) zones (monoatomic layer) - θ″ phase (fully coherent) - θ′ phase (semi-coherent) - θ phase (incoherent) [8-9]. The mechanical properties of Al-Cu alloy can be further enhanced by thermo-mechanical treatment (T8). The pre-deformation was applied between the solution and aging process in T8 treatment, which accelerated the formation of uniformly distributed strengthening phases [10]. The type of the pre-deformation consisted of pre-stretching deformation, cold compression and cold rolling.

Many previous studies on T8 treatment of Al-Cu alloy had been published. He [11] investigated the variation of dissolution for Al_2Cu particles under different cold pre-deformation after solution. The increase of pre-deformation strain was beneficial for an increased number of dissolved Al_2Cu particles and a significant increase in ultimate tensile strength. Li [12] studied the variation of hardness of aged Al–Cu–Mg alloy under different pre-deformations after solution. With the increased pre-deformation, the peak value of the hardness increased and it reached the peak value with a shorter time compared to that without pre-deformation. Meanwhile, the pre-deformation could increase the mechanical properties and shorten the aging time for 2219 forgings [13]. The pre-deformation increased the dislocation density and induced dense θ′ phases with smaller size [14], resulting in further increase of strengths. The pre-deformations were beneficial for the grain size decrease and the change of the distribution of precipitates. Additionally, it also changed the width of precipitation free zone, thus also improving the corrosion resistance of the alloy [15].

A few researches on WAAM deposition of aluminum alloy had also been published. Gomez [16] studied the effects of the parameters on the width, height of one-layer deposition material. Cong [17] and Fang [18] investigated the effect of arc modes in cold metal transfer (CMT) on the porosity of Al-Cu alloy. Pulse and advanced (CMT-PA) was suitable for deposition of aluminum alloy due to its excellent performance in decreasing porosity compared to other CMT modes. Gu [19] integrated inter-layer cold rolling to the WAAM deposition aluminum alloy. The porosity decreased with increased rolling force. Meanwhile, the microstructure was obviously improved and mechanical properties were significantly enhanced with cold rolling process [20].

However, despite the obvious increase of elongation in inter-layer cold rolling, the strengths of cold-rolled Al-Cu alloy after T6 heat treatment were almost the same to that of WAAM deposited [21]. T8 heat treatment was proved to be helpful in increasing the strengths of Al-Cu alloy. Therefore, how to further increase the strengths through different heat treatment and its combination with cold rolling process needed to be further studied. In this study, inter-layer cold rolling followed by T8 treatment was integrated to the WAAM process of 2219 alloy. Meanwhile, the precipitation and fracture morphology were studied. Finally, the strengthening mechanism of the material in inter-layer cold rolling process with T8 treatment was also discussed.

2 Experiments

2.1 Set up of hybrid WAAM deposition and inter-layer rolling

The experimental set up of hybrid WAAM deposition and rolling system is shown in Figure 1. The wire diameter of ER2319 aluminum alloy was 1.2 mm. The WAAM deposition system was made up of a CMT power source (Fronius CMT 4000 advanced), a wire feeder (Fronius, VR 7000), a CMT torch with local shielding device and a 6-axis robot (ABB IRB2400). The cold rolling system consisted of a hydraulic cylinder, a load cell, a flat roller and a CNC system.

The CMT-PA mode was applied due to its advantage of the porosity decrease in as-deposited aluminum alloy [17]. Two comparative walls were built: as-deposited and inter-layer cold-rolled. After the WAAM deposition of one layer, the roller was moved to the top surface of the deposited layer. The rolling force was set to the certain value controlled by the hydraulic cylinder. Compressive rolling deformation was applied on the top surface on each deposited layer through the roller, in which different rolling forces can be adjusted. The inter-layer

cold-rolled samples can be obtained with alternating one-layer deposition and one-layer cold rolling process. The parameters for WAAM deposition and inter-layer cold rolling process were shown in Table 1.

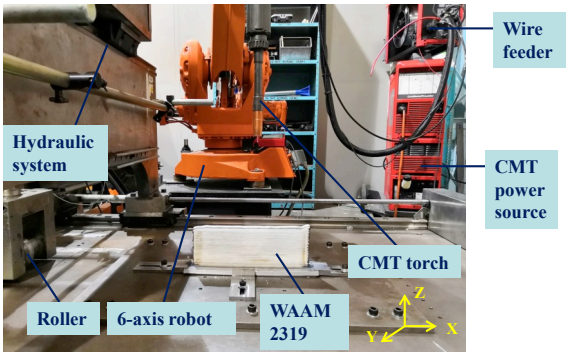


Figure 1 Experimental set up of hybrid WAAM deposition and rolling system

Table 1 Experimental parameters for WAAM deposition and rolling process

Parameter	Value
Contact tip-to-work distance	15 mm
Wire feed speed	6 m/min
Torch travel speed	10 mm/s
Rolling force	0, 45 kN
Roller diameter	100 mm
Roller width	20 mm
Roller travel speed	10 mm/s
Inter-layer cooling time	2 mins
Shielding gas flow rate (pure argon)	25 L/min

2.2 Heat treatments

After the establishment of two comparative walls the effect of heat treatments (T6 and T8 treatment) on microstructure and tensile properties were comparatively investigated. The procedures of T6 treatment were described as follows: solution treatment at 535 ℃ with a ramping speed of 200℃/h and held for 1.5 h in the furnace followed by water quenching; artificial aging treatment at 175℃ with a ramping speed of 100℃/h and held for 3 h followed by furnace cooling. The transfer time from solution treatment to water quenching was less than 10 s due to the sensitivity of quenched aluminum alloy. The pre-stretching deformation of 5% was applied between solution and aging process in T8 treatment using an electro-mechanical tensile machine. Laser extensometer was used to monitor the pre-stretching deformation of the samples. The electro-mechanical tensile machine was immediately stopped when the pre-stretching deformation reached 5%. The temperature and soaking time in T8 were the same with that in T6 treatment.

2.3 Analysis methods

After WAAM deposition and rolling process, samples were cross-sectioned for microstructure observation and hardness measurement. Zwick/Roell hardness tester was adopted with an interval of 1 mm along the vertical direction under a load of 200 g and a holding time of 15 s. Microstructure and second precipitates were observed using an optical microscopy (OM, OPTIPHOT, NIKON) and a scanning electron microscopy (SEM, FEI XL30-SFEG). Meanwhile, element analysis of different precipitates was analyzed using an energy dispersive spectrometry (EDS, OXFORD INSTRUMENTS). The precipitated phases after different heat treatments were observed by a transmission electron microscopy (TEM, FEI Titan G2 60-300).

Tensile coupons were machined along horizontal (X) and vertical (Z) direction of the walls. Tensile tests at room temperature were conducted on an Instron 5500R electro-mechanical machine with a load cell of 30 kN and a crosshead speed of 1 mm/min. Laser extensometer was used to measure the variation of gauge length during the tensile test for the calculation of the elongation. Three samples were tested for each condition and the average value as well as the error bar was obtained.

3 Results and discussions

Table 2 shows the size and strain of as-deposited and cold-rolled walls. The average layer thickness decreased from 2.2 mm in as-deposited condition to 1.24 mm in inter-layer cold-rolled condition with a rolling force of 45 kN. As described by Gu [19], inter-layer rolling with the force of 45 kN shows effective effect in eliminating the porosity of Al-Cu alloy even after heat treatment. The calculation method of strain for each layer was shown in Eq.(1). The strain of 43.6% can be obtained under the inter-layer cold rolling force

of 45 kN. The width of the inter-layer cold-rolled wall increased to 11.7 mm compared to that of 6.5 mm in as-deposited wall. The width of the wall significantly increased during the vertical cold rolling as there was no constraint in the width direction.

$$\varepsilon = \frac{h_{AD} - h_{CR}}{h_{AD}} \times 100\% \quad (1)$$

where hAD is the layer height of WAAM deposition, hCR is the layer height after cold rolling process.

Table 2 Size and strain of as deposited and cold rolled walls

	Layers	Total height (mm)	Average layer height (mm)	Strain (%)	Wall width (mm)
AD	54	118.8	2.20	/	6.50
CR (45kN)	79	97.9	1.24	43.64	11.70

AD: as deposited; CR: cold rolled

3.1 Hardness

Table 3 shows the hardness variation of the as-deposited and cold-rolled samples. There is a hardness increase of 26 HV for the cold-rolled sample compared to that in as-deposited condition. The work hardening induced by the cold rolling process increases the dislocation density inside the material and thereby resulting in a hardness increase. The hardness in the as-deposited sample increases obviously after solution treatment; while there is no distinct hardness increase in the cold-rolled condition. Therefore, the hardness difference between the as-deposited and cold-rolled samples is quite small after solution treatment. The T6 heat treatment significantly increases the hardness for both the as-deposited and cold-rolled samples, indicating that the precipitation strengthening mechanism in the aging treatment contributes to the increase of hardness. However, it can be seen that the hardness difference between as-deposited and cold-rolled samples can be neglected after T6 heat treatment, which is quite difference from that before heat treatment.

Table 3 Hardness variation under different treatments

Hardness	AD	CR
Before heat treatment	74±2.4	100±1.6
Solution	100.7±3.5	102.2±3.8
T6	139.2±4.4	143.7±4.4
T8	152.4±6.7	163.9±4.0

The hardness increases obviously with the pre-stretching strain in T8 treatment and its value is much larger than that in T6 treatment for both the as-deposited and cold-rolled samples. In addition, the hardness difference between the as-deposited and cold-rolled samples in T8 heat treatment is larger than that in T6 heat treatment. It can be inferred that the hardness of the cold-rolled sample increases further with T8 heat treatment and the pre-stretching process plays a vital role in hardness increase.

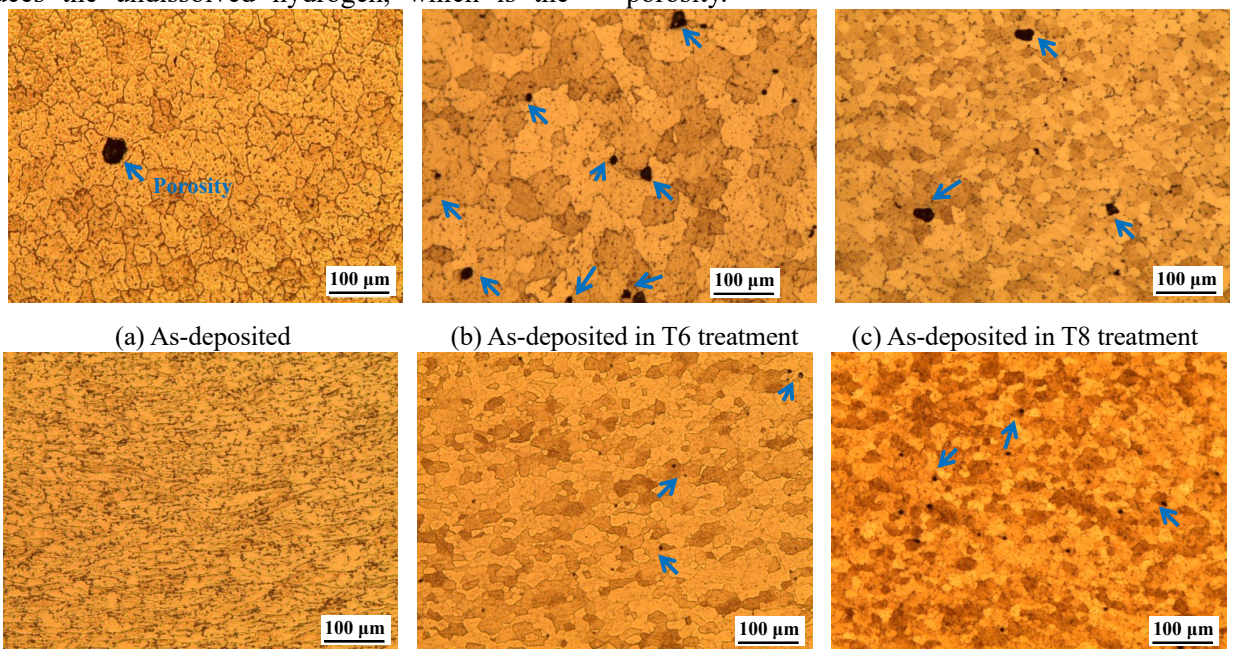
3.2 Microstructure

Figure 2 shows the microstructure with different heat treatments. Fine dendrites and equiaxed grains are formed in as-deposited material due to the low heat input of CMT-PA mode, while the columnar dendrites are more likely to appear in conventional CMT mode. The average grain size of as-deposited sample is 65.4 μm before heat treatment and it increases to 72.8 μm in T6 treatment; however, it decreases drastically to 33.2 μm in T8 treatment.

Fine dendrites and small equiaxed grains change to banded structure in the cold-rolled condition, as shown in Figure 2(d). Meanwhile, the dislocation inside the material obviously increases with the rolling process, thus more deformation energy of the material is accumulated. Sufficient deformation energy and high temperature are essential for the recrystallization process and the grain refinement. With the subsequent new-layer deposition, the transient heat input will trigger the recrystallization process. As a result, the banded structure changes to equiaxed grains. The banded structure changes to equiaxed grains with the average grain size of 58.4 μm after T6 treatment. This is because of the recrystallization process triggered by the heat input from the high temperature in solution treatment. Recrystallized

nuclei appear at grain boundaries of the banded structure and then grow up into recrystallized grains with certain grain size during the solution treatment. Similar to the variation of grain size of as-deposited sample, the average grain size of the cold-rolled sample decreases to 25.1 μm in T8 treatment, which is smaller than that in as-deposited condition.

Although CMT-PA mode is beneficial for porosity reduction in WAAM deposition process, the porosity cannot be completely eliminated with this mode, as shown in Figure 2(a). The T6 treatment increases both the number and the volume fraction of the porosity; while T8 treatment decreases them. The cold rolling process significantly decreases the size and the volume fraction of porosity with a load of 45 kN. Only a few smaller porosities (less than 10 μm) appear after heat treatments, which are quite smaller than that in as-deposited samples. The obvious solubility difference between solute atoms and solvent atoms induces the undissolved hydrogen, which is the main factor for the formation of porosity in solution treatment. The second phase particles (Al_2Cu) are dissolved into the matrix and the dislocation density is recovered at high temperature during solution treatment. According to Anyalebechi's [22] results, the second phase particles and dislocation provide positions for the nucleation of porosity. The dissolution of second phase particles and the decreased dislocation during heat treatment both cause vacant sites inside the material, which contributes to the formation and growth of porosity. As a result, the number and the volume fraction of porosity both increase at high temperature in solution treatment. Wolfer [23] concluded that the solubility of hydrogen increased linearly with the increased dislocation density inside the material. The pre-stretching deformation in T8 treatment plays a vital role in the enhancement of dislocation density, which accelerates the dissolution of hydrogen and decreases the volume fraction of porosity.



(a) As-deposited (b) As-deposited in T6 treatment (c) As-deposited in T8 treatment

(d) Cold-rolled (e) Cold-rolled in T6 treatment (f) Cold-rolled in T8 treatment

Figure 2 Microstructure variation with different heat treatments

Table 4 Tensile test results of 2219 alloy

AD	UTS/MPa	YS/MPa	Elongation (%)	CR	UTS/MPa	YS/MPa	Elongation (%)
Before HT	267.3±2.9	127±3.8	19.2±1.2	Before HT	334.6±5.2	272±2.3	14. 8±1.8
S	373.7±1.4	174.2±5.3	22.3±0.8	S	403.8±1.6	183.7±4.9	30.5±1.2
T6	450.5±11.9	297.4±3.3	13. 9±0.9	T6	458±1.3	292.4±12.8	18.8±4.9
T8	478.9±8.8	384.2±7.2	10.4±0.5	T8	513.4±2.8	412.9±0.1	14.1±1.62

HT: heat treatment; S: solution treatment

3.3 Tensile properties

There is no evident anisotropy of tensile properties for both the as-deposited and cold-rolled 2219 alloy samples [21]. This may be explained in that the low heat input of CMT-PA mode results in equiaxed grains for both the as-deposited and cold-rolled conditions, which is essential for the isotropic tensile properties. Therefore, in this study, only the horizontal tensile test results are investigated, as shown in Table 4. Compared to the as-deposited sample, the cold rolling significantly increases the strengths and reduces the elongation. This suggests that the work hardening induced by the cold rolling process increases the strengths of the material, which in turn decreases the elongation. The solution treatment shows different effect on the variation of the UTS and YS. The solution treatment increases the UTS and elongation for both the conditions. The YS of the as-deposited sample increases in solution treatment, while it decreases for the cold-rolled condition. This may be explained in that the increased dislocation density resulting from the cold rolling process will be recovered at high temperature in solution treatment. The accumulated dislocation density enhances the YS before heat treatment; while the decreased dislocation density may lead to decrease of YS due to the recovery mechanism in solution treatment. It should be noted that the elongation in the cold-rolled sample is larger than that in as-deposited material in solution treatment, which is opposite to that before heat treatment.

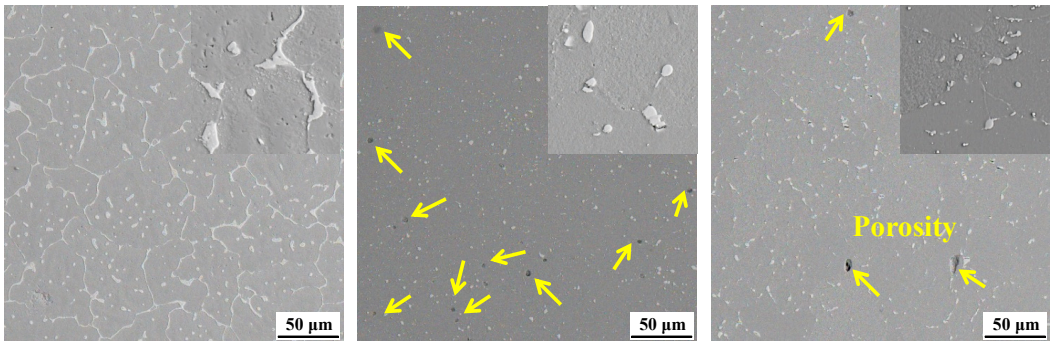
The T6 treatment significantly increases the strengths and decreases the elongation for all samples. As 2219 alloy is a precipitation strengthened alloy, the precipitation in the aging process has significant effect in enhancement of strengths. After T6 treatment, the cold-rolled sample shows larger elongation than that in as-deposited material, while the strengths are almost the same for two conditions.

The strengths can be further increased with slight decrease of elongation in T8 treatment for all samples. UTS of 513 MPa and YS of 412 MPa can be acquired for the cold-rolled samples. It shows comparative strengths or even exceed the strengths of wrought material of 2219 alloy. The elongation of the cold-rolled sample in T8 treatment exceeds or equals to that before heat treatment, indicating that the strengths can be significantly increased without sacrifice of elongation. Therefore, T8 treatment is beneficial for the improvement of the comprehensive tensile properties.

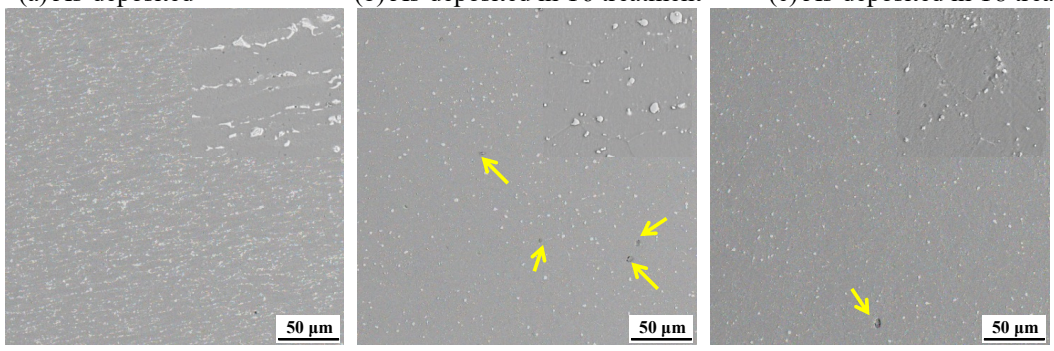
3.4 Precipitation

Figure 3 shows the precipitates distribution for the as-deposited and cold-rolled samples. The white network-like second phases scatter at both grain boundaries and grain interiors for as-deposited condition. The particles are fractured into small pieces and extended in the rolling direction in the cold rolling process. The distribution of the banded-like particles is similar to the banded structure in cold-rolled samples, as shown in Figure 2 (d) and Figure 2 (d).

The T6 treatment decreases the size of the particles and improves the uniformity of the particles distribution for both as-deposited and cold-rolled samples. The size of the particles further decreases in T8 treatment accompanied by the increased volume fraction of particles compared to T6 treatment. The EDS analysis in Figure 4 shows that the white particles are Al-Cu eutectics, and the mass fraction and the atomic fraction of Cu varies in different heat treatments. The mass fraction of Cu is 30.05% without heat treatment, and it changes to 41.52% and 24.93% for T6 and T8 treatment, respectively. Most of the second-phase particles precipitated in WAAM deposition will be dissolved into the matrix in the solution treatment as the solution temperature is close to the Al-Cu eutectic temperature (543 ℃) for 2219 alloy [24]. The dissolved Cu precipitates in the following artificial aging process, resulting in the increased mass fraction of Cu in aging process. However, the mass fraction of Cu in T8 treatment is smaller than that in T6 treatment. This may be explained in that the total content of Cu in the precipitates is constant, large number of precipitated particles decreases the mass fraction of Cu in each measured particle in T8 treatment. In addition, the number of porosity in T6 heat treatment increases compared to that without heat treatment. The heat input from the heat treatment contributes to the growth of the porosities. The quantity of the porosity decreases in T8 treatment and it is consistent with the variation of microstructure results in Figure 2.

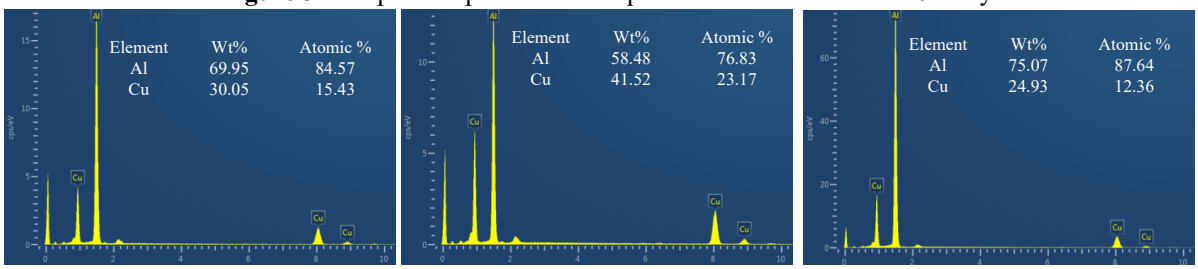


(a) As-deposited (b) As-deposited in T6 treatment (c) As-deposited in T8 treatment



(d) Cold-rolled (e) Cold-rolled in T6 treatment (f) Cold-rolled in T8 treatment

Figure 3 Precipitation phases in as-deposited and cold-rolled 2219 alloy



(a) Without heat treatment (b) T6 heat treatment (c) T8 heat treatment

Figure 4 Energy dispersive spectrometry (EDS) analysis of precipitates

3.5 Fracture morphology

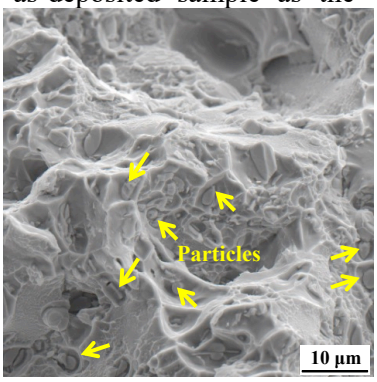
The fracture surfaces of the tensile samples after T6 and T8 treatments are shown in Figure 5. The angle between the fracture surfaces and the tensile load direction is near 45°, indicating shear fracture mode appears for all the samples in T6 and T8 treatments. According to elastic-plastic mechanics theory, the angle between the maximum shear stress and the principal stress is 45° in theory, in which the principal stress is equal to the tensile stress in uniaxial tensile test.

The fracture morphology of the tensile samples is examined with SEM, as shown in Figure 6. Coarser and deeper dimples with second phase particles inside the particles (marked with yellow arrow) are exhibited in T6 treatment of the as-deposited sample, indicating that the trans-granular ductile fracture mode is generated, as shown in Figure 6(a). The number of dimples increases accompanied by the decreased dimples size in the cold-rolled surface, thus contributing to the formation of uniformly distributed dimples and a higher elongation. According to the EDS analysis, these particles are proved to be Al-Cu eutectics. Primary crack could be initiated in these places as the particles provide positions for the formation, coalescence and propagation of microvoids. Smaller and shallower dimples as well as a few islands of flat surface are exhibited for both conditions in T8 treatment, showing a brittle fracture characteristic. Meanwhile, there are some porosities and secondary cracks for both the as-deposited and cold-rolled materials. The fracture characteristic, porosity and secondary cracks in T8 treatment lead to the decreased elongation compared to that in T6 treatment. The microvoids preferentially appear at the positions of porosity and second phase particles. The microvoids nucleation

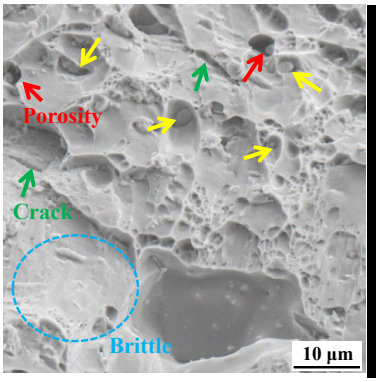
is triggered when the elastic energy of the newly formed microvoid positions is smaller than that of the second phase particles. The propagated secondary crack resulting from microvoid coalescence may eventually cause inter-granular ductile fracture. Meanwhile, the interaction between the sheared second phase particles and the high resolved shear stress during tensile test may induce the trans-crystalline localization [25]. Therefore, the locally ductile and brittle failure features in T8 treatment may further decrease the elongation. Nevertheless, the quantity of porosity and secondary crack is lower for the cold-rolled surface compared to that in as-deposited sample as the rolling process contributes to the closure of the porosity and the crack.



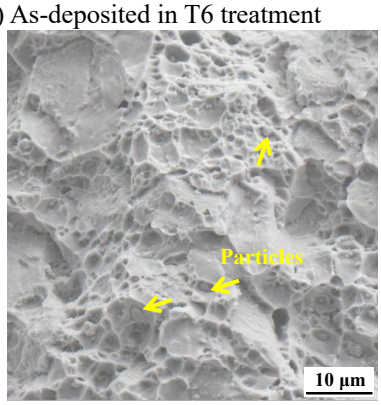
Figure 5 Fracture specimens after T6 and T8 heat treatments



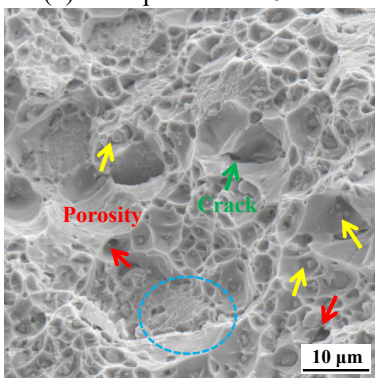
(a) As-deposited in T6 treatment



(b) As-deposited in T8 treatment



(c) Cold-rolled in T6 treatment



(d) Cold-rolled in T8 treatment

Figure 6 Fracture morphology after T6 and T8 treatment

3.6 Strengthening mechanism

As shown in Table 3, the cold rolling process significantly increases the hardness compared to the as-deposited sample. The dislocation density increases in the cold rolling process, which induced by the work hardening. Meanwhile, the hardness also increases after solution treatment; this was induced by the solution strengthening. Supersaturated solid solution will be generated during solution treatment, and the interaction between the solute atoms and dislocation may impede the motion of dislocation and increase the strengths of the material.

After the solution treatment followed by the pre-stretching process, the hardness for as-deposited and cold-rolled samples is 112 HV and 115 HV, respectively. The hardness increment for as-deposited sample is 12 HV induced by the pre-stretching process. Meanwhile, the hardness increment is 13 HV from T6 to T8 treatments for as-deposited sample. It is interesting that the hardness increment from T6 to T8 treatments is equal to that induced by the pre-stretching process in the as-deposited sample. The hardness increment

in cold-rolled sample induced by the pre-stretching process is 13 HV, which almost equals to that in as-deposited samples. Therefore, the strain induced strengthening in the pre-stretching process contributes to the equal hardness increase for both conditions. Nevertheless, the hardness increment from T6 to T8 treatments in cold-rolled sample is 20 HV. This increment is larger than that induced by the pre-stretching process, indicating that the strengthening mechanism in cold-rolled condition is different from that in as-deposited samples. This may be explained as follows: there is a dynamic variation of dislocation density for the cold-rolled sample in T8 treatment. The dislocation density first increases in the cold rolling process before heat treatment; then it decreases due to the recovery at solution treatment and finally it increases again in the pre-stretching process. The complicated variation of dislocation density in the cold-rolled sample leads to the change of hardness.

It is interesting that the strengths in the as-deposited and cold-rolled samples with T6 treatment are almost the same. However, the average grain size in two conditions is quite different, as shown in Figure 2. According to the Hall-Petch relationship, the strength of the material is in inverse to the average grain size. It can be inferred that the grain boundary strengthening is not the predominant strengthening mechanism for 2219 alloy.

Table 5 Tensile results with solution treatment followed by pre-stretching process

	UTS/MPa	YS/MPa	Elongation (%)
AD	397.3±0.4	317.7±2.5	16±0.9
CR	413.5±5.5	339.4±8.3	18.8±1.8

To investigate the effect of pre-stretching process on the strengths variation, the tensile properties with solution treatment followed by pre-stretching process are measured, as shown in Table 5. The pre-stretching strain between solution and aging treatment shows a pronounced increase of YS and a slight increase of UTS for both conditions. Similar to the variation of hardness, the pre-stretching strain plays the equal effect on the increase of YS for both conditions. The UTS increment from T6 to T8 treatments is the same with that from solution to pre-stretching process in as-deposited samples. However, the UTS increment from T6 to T8 treatments is much larger than that induced by the pre-stretching process in cold-rolled sample.

The precipitation of strengthening phases is examined by TEM, which is an effective method for the analysis of the strength variation. As shown in Figure 7, there are dislocation lines and tangled dislocations with some acicular precipitated phases around the dislocations in T6 treatment. The density and area fraction of tangled dislocations significantly increase, meanwhile, the tangled dislocations transform to dislocation cells and dislocation rings in T8 treatment. It can be inferred that the pre-stretching process contributes to the aggregation and slippage of the dislocation in the matrix of the material, thus leading to the increased dislocation density. The increased dislocation provides potential favorable positions for the precipitated phases due to its high free energy, the nucleation of these phase and its growth are more likely to occur at these positions.

T6 treatment leads to heterogeneous distribution of the strengthening phases as some parts are densely distributed around the dislocations while others are sparse precipitated, as shown in Figure 8 (a). The acicular phases with the length of 70~166 nm prove to be θ′ phases according to the corresponding selected area electron diffraction (SAED) profile along the {110} Al direction. There are large amounts of tiny and dense precipitates around the θ′ phases, which is θ″ phases based on the discontinuous streaks in the SAED pattern along {020} Al direction. It can be seen that θ″ phases are the main strengthening phases in T6 treatment due to its high area fraction compared to that of θ′ phases. T8 treatment shows dense and dispersive distributed θ′ phase and its area fraction is significantly increased compared to the T6 treatment, which can be deduced from the obvious increase in the streak intensity along the {110} Al direction as shown in Figure 8 (b). It is obvious that some portions of θ″ phases have transformed into θ′ phases in T8 treatment and θ′ phases are the main strengthening phases.

T8 treatment shows denser strengthening phases with more dispersive distribution compared to that in T6 treatment, which contributes significantly to the further increase of strengths. The strengthening mechanisms for T8 heat treatment are summarized as follows: first, both the

cold rolling process and pre-stretching strain increases the dislocation density inside the material. The accumulated dislocation density increases the strengths of the material; that is the work hardening. Secondly, the increased dislocations provide more preferential positions for the nucleation of the θ′ phase and accelerate its formation; as a result, the increased nucleation rate increases the volume fraction of the θ′ phase and reveals a dense distribution of θ′ phases. The dense and uniformly distributed strengthening precipitates will pin up the dislocations and inhibit the movement of dislocation, thus significantly increasing the strengths of the material. Thirdly, according to Ma's study [26], the metastable plate-like θ′ phases show a higher shear resistance than the θ″ phases. Therefore, larger volume fraction of θ′ phases after T8 treatment plays a more effective role in enhancing the strengths of the material compared to the dense distribution of θ″ phases after T6 treatment. Finally, the formation of massive solute atom atmospheres can be promoted due to the increased dislocation density and the accelerated interaction between extensive solute atoms and moving dislocation. The formation of massive solute atom atmospheres also contributes to the enhancement of strength as they can also be the nucleation sites for precipitated phases [27].

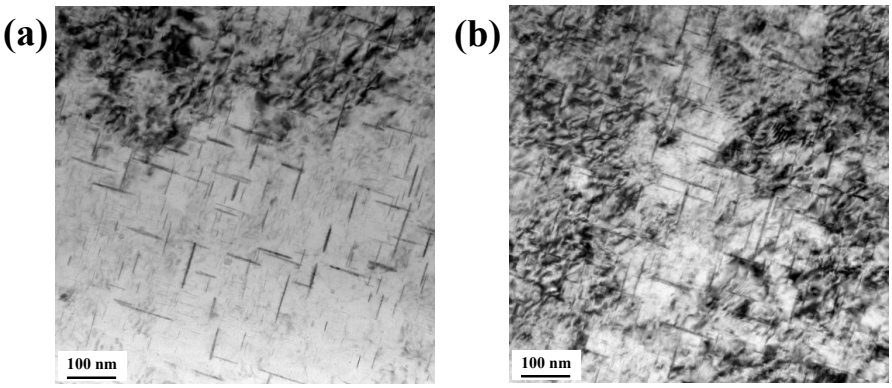


Figure 7 TEM micrographs of : (a) T6 heat treatment and (b) T8 heat treatment

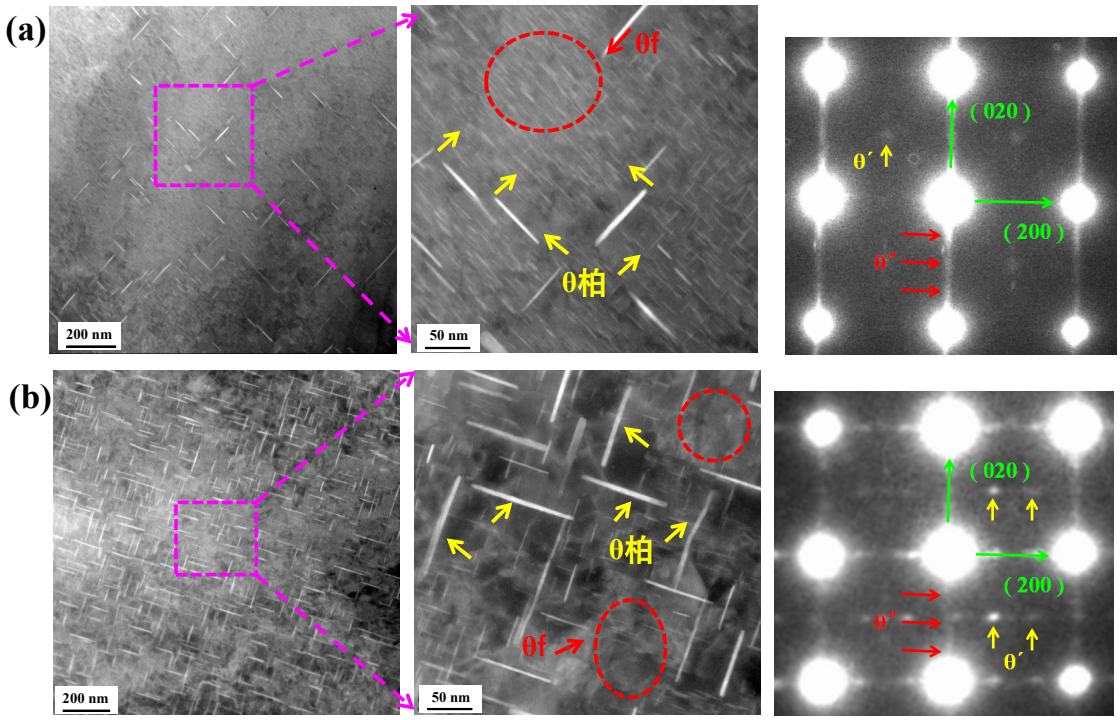


Figure 8 Precipitates distribution of : (a) T6 heat treatment and (b) T8 heat treatment

4 Conclusions

Inter-layer cold rolling was integrated to the WAAM deposition process. The effects of T6 and

T8 treatments on the microstructure and mechanical properties were comparatively investigated.

1. The inter-layer cold rolling increases the hardness and strengths, and decreases the elongation before heat treatment.
2. The heat treatments increase the strengths and reduce the elongation. The cold-rolled samples show larger strengths and higher elongation after T8 treatment compared to that in as-deposited condition.
3. Fine dendrites and equiaxed grains change to banded structure in the cold rolling process, and it transforms to smaller equiaxed grains after heat treatment. The average grain size can be further decreased in T8 treatment.
4. Cold rolling and pre-stretching deformation both increase the dislocation density, and contribute to the formation of tiny and dense θ′ phases with dispersive distribution, thus significantly enhancing the strengths. T8 treatment shows better strengthening effect than the T6 treatment.
5. Shear fracture and trans-granular ductile fracture mode are the main characteristic for samples with T6 treatment; while trans-granular ductile fracture mode with a brittle fracture characteristic appear on the fracture surface after T8 treatment.
6.The main strengthening mechanisms of T8 heat treatment are precipitation strengthening and strain induced strengthening.

Contributors

Tao Zhang: Conceptualization, Writing – original draft. Zhenyang Qin: Experiment and analysis. Hai Gong: Supervision, Writing – review & editing. Yunxin Wu: Proof reading and revision. Xin Chen: Investigation.

Conflict of interest

The authors declare that they have no known competing financial interests or personal relationships that could have appeared to influence the work reported in this paper.

References

[1] AN Li-hui, CAI Yang, LIU Wei, YUAN Shi-jian, ZHU Shi-qiang, MENG Fan-cheng. Effect of pre-deformation on microstructure and mechanical properties of 2219 aluminum alloy sheet by thermomechanical treatment[J]. Transactions of Nonferrous Metals Society of China, 2012, 22: 370-375.

[2] LIU Lei, WU Yun-xin, GONG Hai, LI Shuang, AHMAD A. A Physically Based Constitutive Model and Continuous Dynamic Recrystallization Behavior Analysis of 2219 Aluminum Alloy during Hot Deformation Process[J]. Materials, 2018, 11: 1443-1457.

[3] LOCKETT H, DING J, WILLIAMS S, MARTINA F. Design for wire + arc additive manufacture: design rules and build orientation selection[J]. Journal of Engineering Design, 2017, 3: 1-31.

[4] SHEN Chen, PAN Zeng-xi, CUIURI D, ROBERTS J, LI Hui-jun. Fabrication of Fe-FeAl Functionally Graded Material Using the Wire-Arc Additive Manufacturing Process[J]. Metallurgical and Materials Transactions B, 2016,47: 763-772.

[5] WILLIAMS S, MARTINA F, ADDISON A, DING J, PARDAL G, COLEGROVE P. Wire + arc additive manufacturing[J]. Materials Science and Technology, 2016, 7: 641-647.

[6] ASALA G, KHAN A, ANDERSSON J, OJO O. Microstructural Analyses of ATI 718Plus®, Produced by Wire-ARC Additive Manufacturing Process[J]. Metallurgical and Materials Transactions A, 2017, 48: 4211-4228.

[7] ZHANG Deng-kui, LI Quan, ZHAO Yue, LIU Xian-li, SONG Jian-ling, WANG Guo-qing, WU Ai-ping. Microstructure and Mechanical Properties of Three-Layer TIG-Welded 2219 Aluminum Alloys with Dissimilar Heat Treatments[J]. Journal of Materials Engineering and Performance, 2018, 27: 2938-2948.

[8] TAO Jia-shen, ZHANG Liang, WU Guo-hua, CHEN An-tao, ZHANG Xiao-long, SHI Chun-chang. Effect of heat treatment on the microstructure and mechanical properties of extruded Al-4Cu-1Li-0.4Mg-0.4Ag-0.18Zr Alloy[J]. Materials Science and Engineering: A, 2018, 717: 11–19.

[9] JOSHI A, YOGESHA K, JAYAGANTHANA R. Influence of cryorolling and followed by annealing on high cycle fatigue behavior of ultrafine grained Al 2014 alloy[J]. Materials Characterization, 2017, 127: 253–271.

[10] LI Xi-feng, LEI Kun , SONG Peng, LIU Xin-qin, ZHANG Fei , LI Jian-fei , CHEN Jun. Strengthening of aluminum alloy 2219 by thermo-mechanical treatment[J]. Journal of Materials Engineering and Performance, 2015, 24: 3905-3911.

[11] HE Hai-lin, YI You-ping, HUANG Shi-quan, ZHANG Yu-xun. Effects of cold predeformation on dissolution of second-phase Al_2Cu particles during solution treatment of 2219 Al-Cu alloy forgings[J]. Materials Characterization, 2018, 135: 18-24.

[12] LI Hui-zhong, LIU Ruo-mei, LIANG Xiao-peng, DENG Min, LIAO Hui-juan, HUANG Lan. Effect of pre-deformation on microstructures and mechanical properties of high purity Al–Cu–Mg alloy[J]. Transactions of Nonferrous Metals Society of China, 2016, 26: 1482-1490.

[13] WANG Hui-min, YI You-ping, HUANG Shi-quan. Influence of pre-deformation and subsequent ageing on the hardening behavior and microstructure of 2219 aluminum alloy forgings[J]. Journal of Alloys and Compounds, 2016, 685: 941-948.

[14] LU Ya-lin, WANG Jian, LI Xing-cheng, CHEN Yi, ZHOU

Dong-shuai, ZHOU Gang, XU Wen-ting. Effect of pre-deformation on the microstructures and properties of 2219 aluminum alloy during aging treatment[J]. Journal of Alloys and Compounds, 2016, 699: 1140-1145.

[15] LU Ya-lin, WANg Jian, LI Xing-cheng, LI Wen, LI Ruo-lin, ZHOU Dong-shuai. Effects of pre-deformation on the microstructures and corrosion behavior of 2219 aluminum alloys[J]. Materials Science and Engineering: A, 2018, 723: 204-211.

[16] GOMEZ ORTEGA A, CORONA GALVAN L, DESCHAUX-BEAUME F, MEZRAG B, ROUQUETTE S. Effect of process parameters on the quality of aluminium alloy Al5Si deposits in wire and arc additive manufacturing using a cold metal transfer process[J]. Science and Technology of Welding and Joining, 2017, 23: 1-17.

[17] CONG Bao-qiang, DING Jia-luo, WILLIAMS S. Effect of arc mode in cold metal transfer process on porosity of additively manufactured Al-6.3%Cu alloy[J]. The International Journal of Advanced Manufacturing Technology, 2015, 76: 1593-1606.

[18] FANG Xue-wei, ZHANG Li-juan, LI Hui, LI Chao-long, HUANG Ke, LU Bing-heng. Microstructure Evolution and Mechanical Behavior of 2219 Aluminum Alloys Additively Fabricated by the Cold Metal Transfer Process[J]. Materials, 2018, 11: 812-824.

[19] GU Jiang-long, DING Jia-luo, WILLIAMS S, Gu Hui-min, MA Pei-hua , ZHAI Yu-chun. The effect of inter-layer cold working and post-deposition heat treatment on porosity in additively manufactured aluminum alloys[J]. Journal of materials processing technology, 2016, 230: 26-34.

[20] GU Jiang-long, WANG Xiao-shu, BAI Jing, DING Jia-luo, WILLIAMS S, ZHAI Yu-chun, LIU Kun. Deformation microstructures and strengthening mechanisms for the wire+arc additively manufactured Al-Mg4.5Mn alloy with inter-layer rolling[J]. Materials Science and Engineering: A, 2018, 712: 292-301.

[21] GU Jiang-long, DING Jia-luo, WILLIAMS S, GU Hui-min, BAI Jing, ZHAI Yu-chun, MA Pei-hua. The strengthening effect of inter-layer cold working and post-deposition heat treatment on the additively manufactured Al-6.3Cu alloy[J]. Materials Science and Engineering: A, 2015, 651: 18-26.

[22] ANYALEBECHI P, HOGARTH J. Effect of supereutectic homogenization on incidence of porosity in aluminum alloy 2014 ingot[J]. Metallurgical and Materials Transactions B, 1994, 25: 111–122.

[23] WOLFER W, BASKES M. Interstitial solute trapping by edge dislocations[J]. Acta Metallurgica, 1985, 33: 2005-2011.

[24] HORN V, ROBERTSON K. Aluminum: Properties, Physical Metallurgy and Phase Diagrams[M]. American Society for Metals, 1967.

[25] LI Xi-feng, LEI Kun, SONG Peng, LIU Xin-qin, ZHANG Fei , LI Jian-fei , CHEN Jun. Strengthening of aluminum alloy 2219 by thermo-mechanical treatment[J]. Journal of Materials Engineering and Performance, 2015, 24: 3905-3911.

[26] MA P, LIU C, WU C, LIU L, CHEN J. Mechanical properties enhanced by deformation-modified precipitation of θ′-phase approximants in an Al-Cu alloy[J]. Materials Science and Engineering: A, 2016, 676:138–145.

[27] YOSHIMURA R, KONNO T, ABE E, HIRAGA K. Transmission electron microscopy study of the early stage of precipitates in aged Al–Li–Cu alloys[J]. Acta Materialia, 2003, 51: 2891-2903.

(Edited by HE Yun-bin)

中文导读

形变热处理对电弧增材铝-铜合金微观组织及力学性能影响研究

摘要：电弧增材制造技术在铝-铜合金构件制造中极具潜力，然而增材制造构件较低的力学性能限制了其在工业中的应用。本文将层间冷轧和形变热处理（T8）同时集成到电弧增材铝-铜合金中，通过在固溶和时效工艺过程中添加预拉伸变形实现形变热处理。本文研究了形变热处理和层间冷轧对构件硬度、微观组织和力学性能的影响规律，并与传统 T6 热处理进行了对比分析。结果表明层间冷轧可以提升材料硬度和强度，形变热处理可进一步提升其数值。结合层间冷轧和 T8 热处理，可获得 513 MPa 抗拉强度和 413 MPa 屈服强度的试件，这远高于电弧增材态试件。与电弧增材态试样相比，层间冷轧能显著消减气孔，获得更高的延伸率。层间冷轧和 T8 热处理均有利于形成细小弥散分布的 θ′析出相，有利于阻碍位错运动，提升强度，T8 热处理能获得比传统 T6 热处理更好的强化效果。本文讨论了层间冷轧和 T8 热处理综合作用下的强化机制，主要取决于材料的加工硬化和析出强化机制。

关键词：电弧增材；层间冷轧；形变热处理；微观组织；力学性能；强化机制



https://dspace.org/

Effect of thermo-mechanical treatment on microstructure and mechanical properties of wire-arc additively manufactured Al-Cu alloy

Zhang, Tao; Qin, Zhen-yang; Gong, Hai; Wu, Yun-xin; Chen, Xin

2024-07
Springer
https://doi.org/10.1007/s11771-024-5740-2
Zhang T, Qin Z-Y, Gong H, et al., (2024) Effect of thermo-mechanical treatment on microstructure and mechanical properties of wire-arc additively manufactured Al-Cu alloy. Journal of Central South University, Volume 31, Issue 7, July 2024, pp. 2181-2193

Downloaded from a DSpace repository. https://dspace.org/